Proceedings of the 17th World Congress
The International Federation of Automatic Control
Seoul, Korea, July 6-11, 2008

Asymptotic Stability of Hierarchical Inner-Outer Loop-Based Flight Controllers

Farid Kendoul *, **Isabelle Fantoni** ** and **Rogelio Lozano** ***

* *Laboratoire Heudiasyc, CNRS-UTC, 60200 Compiègne, France (Tel: 00333 44 23 49 54; e-mail: fkendoul@hds.utc.fr).*
** *(e-mail: ifantoni@hds.utc.fr)*
*** *(e-mail: rlozano@hds.utc.fr)*

Abstract: In this paper, we present a hierarchical controller for autonomous aerial vehicles control and navigation. For autonomous rotorcraft flight, it is common to separate the flight control problem into an inner loop that controls attitude and an outer loop that controls the translational trajectory of the rotorcraft. The resulted nonlinear controller is thus, easy to implement and to tune. Although satisfactory results have been reported in the literature and various navigational tasks have been achieved using this hierarchical control technique, this control scheme suffers from the lack of the stability proof and analysis of the closed-loop system. Here, we propose a 3D flight controller which is based on the inner- and outer-loop control scheme, and we prove the asymptotic stability property for the connected closed-loop system.

Keywords: Rotorcraft control, hierarchical control, stability analysis, systems in cascade.

1. INTRODUCTION

Although the research on Unmanned Aerial Vehicles (UAVs) goes back to the last decade, the UAV control has a rich literature with different control techniques. Conventional approaches to UAV flight control involve dynamics linearization about a set of pre-selected equilibrium conditions or trim points, La Civita et al. (2006). Then, many linear control techniques such as classical PID, Bouabdallah et al. (2004), can be applied. However, these approaches suffer from performance degradation when the aircraft moves away from a design trim point. Hence, gain scheduling is usually required to obtain acceptable performance, Oosterom and Babuska (2006). The main drawback of this approach is the severe trade-off between control performance and the number of the required trim points.

In order to overcome some of the limitations and drawbacks of the previous linear approaches, a variety of nonlinear flight control techniques have been developed. Among these, feedback linearization, Koo and Sastry (1998), dynamic inversion, Reiner et al. (1995); Johnson and Kannan (2005) and backstepping, Olfati-Saber (2001); Mahony and Hamel (2004) techniques have received much of the attention and showed great promise. However, few controllers have been successfully implemented and tested on real aircraft for achieving realistic navigational tasks. The most popular flight controllers that have achieved quite good performances in real flights are those based on the inner- and outer-loop control scheme. In designing these practical controllers, the conventional conceptual separation between the position (outer-loop) and the orientation (inner-loop) is made Johnson and Kannan (2005); La Civita et al. (2006); Nonami (2006).

Most rotary-wing aerial vehicles are under-actuated mechanical systems with six degrees of freedom and four control inputs, which generally include the total thrust and three control torques. The total thrust is used to compensate the gravity force and to control the vertical movement. The horizontal movements are controlled by directing the force vector in the appropriate direction (thrust vectoring control). The control moments are thus used to control the aircraft body orientation which controls the rotorcraft horizontal movement. Therefore, some flight controllers take advantage of rotorcraft model structure and separate the control design into an inner-loop that controls the moments acting on the aircraft, and an outer-loop that controls the thrust force acting on the aircraft. In fact, the thrust vector is effectively oriented in the desired direction by controlling changes to the UAV attitude using the inner-loop. This hierarchical control scheme is motivated by several reasons and has many advantages. Firstly, it is suitable for rotorcraft UAVs control because of their models structure. Secondly, the obtained flight controllers are simple, easy to implement and to tune. Finally, most of the aerospace systems (spacecraft, launchers, aircraft, UAVs) use this hierarchical control scheme for many years, and satisfactory results have been obtained.

The idea of controlling the rotorcraft position through its orientation has been exploited by many researchers. The most popular control techniques using this methodology are the backstepping and dynamic inversion-based flight controllers.

When applying the backstepping methodology to UAVs, the control design is usually based on the following model

⋆ This work was supported by the Picardie Region Council

(see Olfati-Saber (2001); Mahony and Hamel (2004); Kendoul et al. (2006)):

$$\begin{cases} \dot{\xi} = v \\ \dot{v} = \dfrac{1}{m} RF - ge_3 \\ \dot{R} = R\,\mathrm{sk}(\Omega) \\ \dot{\Omega} = J^{-1}\tau - J^{-1}\Omega \times J\Omega \end{cases} \tag{1}$$

The control laws are then constructed in four steps. The resulted control algorithms are somewhat complex and difficult to implement. Indeed, the obtained control laws are coupled and they are not given explicitly. Therefore, the adjustment of controller parameters is not trivial, especially when the plant parameters are not known. The main advantage of the backstepping approach is the proof of the closed-loop system stability, Mahony and Hamel (2004); Sepulcre et al. (1997); Olfati-Saber (2001); Kendoul et al. (2006); Hamel et al. (2002).

On the other hand, the dynamic inversion technique is usually applied to the transformed model given by the following equations (see Section 2):

$$\begin{cases} \ddot{\xi} = \nu + \Delta_\xi(\xi, \dot{\xi}, \eta) \\ \ddot{\eta} = \tilde{\tau} + \Delta_\eta(\xi, \dot{\xi}, \eta, \dot{\eta}) \end{cases} \tag{2}$$

where $(\nu, \tilde{\tau}) \in \mathbb{R}^6$ are the desired control vectors and $(\Delta_\xi, \Delta_\eta) \in \mathbb{R}^3 \times \mathbb{R}^3$ are the model inversion errors. Thus, the control design is achieved in two steps: 1) synthesize a control law for the ξ-subsystem (outer-loop); and 2) design a second control law for the η-subsystem (inner-loop). It is clear that the control design is very simple in this case and the obtained controller is easy to implement and to tune. The major drawback of this approach is the loss of the closed-loop system stability. Indeed, the existing controllers suffer from the lack of stability analysis and robustness with respect to model inversion errors $(\Delta_\xi, \Delta_\eta)$. Some researchers have tried to overcome this issue by incorporating an adaptive term in the control law for compensating the model inversion errors, Johnson and Kannan (2005). Once again, the asymptotic stability of the connected system (2) is not guaranteed.

In this paper, we present the main steps for designing a hierarchical flight controller that is based on the inner-outer loop control scheme. Our objective is to design a 3D flight control system that performs well in practice as well as in theory. Indeed, a control system is required to be practical for real-world applications while guaranteeing the stability of the closed-loop system. To reach this goal, we have separated the aircraft model into two connected subsystems by exploiting the structural properties of rotorcraft UAVs model. The outer-loop with slow dynamics which controls the position, and the inner-loop with fast dynamics which controls the orientation. Thus, each subsystem can be controlled independently using linear or/and nonlinear control tools. The asymptotic stability of the entire connected system is proven by exploiting the theories of systems in cascade.

In Section 2, we recall the dynamic model of rotorcraft UAVs and formulate the control problem as the control of two systems in cascade. Section 3 is devoted to the presentation of some theorems about the stability of systems in cascade. Section 4 is devoted to the control design and the analysis of the closed-loop system stability. In section 5, we show simulation results for stabilization and trajectory tracking. Some concluding remarks are given in Section 6.

2. PROBLEM STATEMENT

The dynamics of a rotorcraft UAV such as the quadrotor helicopter can be represented by the following mathematical model, Kendoul et al. (2007); Olfati-Saber (2001):

$$\begin{cases} \ddot{\xi} = \dfrac{1}{m} uRe_3 - ge_3 \\ M(\eta)\ddot{\eta} + C(\eta, \dot{\eta})\dot{\eta} = \Psi(\eta)^T \tau \end{cases} \tag{3}$$

where ξ and η are the aircraft position and orientation respectively. (u, τ) are the applied thrust and torque vector, R and Ψ are the rotation matrix and Euler matrix respectively. The pseudo inertial matrix M is defined as $M(\eta) = \Psi(\eta)^T J \Psi(\eta)$, and the centripetal vector C is given by $C(\eta, \dot{\eta}) = \Psi(\eta)^T J \dot{\Psi}(\eta) - \Psi(\eta)^T sk(\Psi(\eta)\dot{\eta}) J \Psi(\eta)$.

Since the attitude dynamics in (3) is a fully-actuated mechanical system for $\theta \neq k\pi/2$, then it is exact feedback linearizable. In fact, by considering the following change of variables:

$$\tau = J\Psi(\eta)\tilde{\tau} + \Psi^{-1} C(\eta, \dot{\eta})\dot{\eta} \tag{4}$$

we obtain a 3-dimensional double-integrator. Hence, the system (3) can be written in the following form:

$$\begin{cases} \ddot{\xi} = \dfrac{1}{m} uRe_3 - ge_3 \\ \ddot{\eta} = \tilde{\tau} \end{cases} \Rightarrow \begin{cases} \ddot{x} = -\dfrac{1}{m} u \sin(\theta), & \ddot{\phi} = \tilde{\tau}_\phi \\ \ddot{y} = \dfrac{1}{m} u \cos(\theta)\sin(\phi), & \ddot{\theta} = \tilde{\tau}_\theta \\ \ddot{z} = \dfrac{1}{m} u \cos(\theta)\cos(\phi) - g, & \ddot{\psi} = \tilde{\tau}_\psi \end{cases} \tag{5}$$

Unlike some standard backstepping approaches where the control law is constructed in four steps, the backstepping principle is here applied to transform system (5) into two subsystems in cascade.

Let us first, define a virtual control vector $\nu \in \mathbb{R}^3$ as follows:

$$\nu = q(u, \phi_d, \theta_d) = \frac{1}{m} uR(\phi_d, \theta_d)e_3 - ge_3 \tag{6}$$

where $q(.) : \mathbb{R}^3 \to \mathbb{R}^3$ is a continuous invertible function and (ϕ_d, θ_d) is the desired roll and pitch angles. Hence, $(u, \phi_d, \theta_d)^T = q^{-1}(\nu)$. More precisely, by using the expression of the matrix R, the pseudo-control vector components can be defined as follows:

$$\begin{cases} \nu_x = -\dfrac{1}{m} u \sin(\theta_d) \\ \nu_y = \dfrac{1}{m} u \cos(\theta_d)\sin(\phi_d) \\ \nu_z = \dfrac{1}{m} u \cos(\theta_d)\cos(\phi_d) - g \end{cases} \Rightarrow \begin{cases} u = m\sqrt{\nu_x^2 + \nu_y^2 + (\nu_z + g)^2} \\ \phi_d = \tan^{-1}\left(\dfrac{\nu_y}{\nu_z + g}\right) \\ \theta_d = \sin^{-1}\left(\dfrac{-\nu_x}{\sqrt{\nu_x^2 + \nu_y^2 + (\nu_z + g)^2}}\right) \end{cases} \tag{7}$$

Since the angles (ϕ, θ, ψ) are the state variables of the orientation subsystem, then the desired angles $(\phi_d, \theta_d, \psi_d)$ can not be provided instantaneously. We will then define the following error vector $e = (e_\eta, e_{\dot{\eta}})^T \in R^6$ such that $e_\eta = \eta - \eta_d$ and $e_{\dot{\eta}} = \dot{\eta} - \dot{\eta}_d$. The vector η_d contains the desired Euler angles which are ϕ_d, θ_d (see equ. (7)) and ψ_d which is a reference trajectory given by the user or by a high-level navigation system.

Now, by replacing (ϕ, θ) in (5) by $(\phi_d + e_\phi, \theta_d + e_\theta)$, the system (5) can be written in the following form:

$$\begin{cases} \dot{\xi} = \upsilon, \qquad \dot{\upsilon} = \nu + \dfrac{1}{m} u\, h(\eta_d, e_\eta) \\ \dot{e}_\eta = e_{\dot{\eta}}, \quad \dot{e}_{\dot{\eta}} = \tilde{\tau} - \ddot{\eta}_d \end{cases} \tag{8}$$

The components of the interconnection term $h = (h_x, h_y, h_z)^T$ are given by:

$$\begin{cases} h_x = -[\sin(e_\theta/2)\cos(\theta_d + e_\theta/2)] \\ h_y = [h_1(.)h_2(.) + \sin\phi_d h_2(.) + \cos\theta_d h_1(.)] \\ h_z = [h_2(.)h_3(.) + \cos\phi_d h_2(.) + \cos\theta_d h_3(.)] \\ \text{and} \\ h_1 = \sin(e_\phi/2)\cos(\phi_d + e_\phi/2) \\ h_2 = -\sin(e_\theta/2)\sin(\theta_d + e_\theta/2) \\ h_3 = -\sin(e_\phi/2)\sin(\phi_d + e_\phi/2) \end{cases} \tag{9}$$

Remark 1. When computing the explicit expressions of the interconnection term $h(\eta_d, e_\eta)$, we have exploited some useful relations between trigonometric functions such as:

$$\begin{cases} \sin(a+b) = \sin(a) + \sin(b/2)\cos(a + b/2) \\ \cos(a+b) = \cos(a) - \sin(b/2)\sin(a + b/2) \end{cases} \tag{10}$$

By defining the tracking errors $\chi = (\xi - \xi_d, \upsilon - \upsilon_d)^T \in \mathbb{R}^6$ and $e = (e_\eta, e_{\dot{\eta}})^T \in \mathbb{R}^6$, the system (8) becomes:

$$\begin{cases} \dot{\chi} = \underbrace{A_1\chi + B_1(\nu - \ddot{\xi}_d)}_{f(\chi,\nu,\ddot{\xi}_d)} + \underbrace{\dfrac{1}{m} u\, H(\eta_d, e_\eta)}_{\Delta(u,\eta_d,e_\eta)} \\ \dot{e} = A_2 e + B_2(\tilde{\tau} - \ddot{\eta}_d) \end{cases} \tag{11}$$

where $H(\eta_d, e_\eta) = (0, 0, 0, h_x, h_y, h_z)^T$. The matrices $A_1 \in \mathbb{R}^{6\times6}, B_1 \in \mathbb{R}^{6\times3}, A_2 \in \mathbb{R}^{6\times6}$ and $B_2 \in \mathbb{R}^{6\times3}$ are defined as follows:

$$A_1 = A_2 = \begin{bmatrix} 0&0&0&1&0&0 \\ 0&0&0&0&1&0 \\ 0&0&0&0&0&1 \\ 0&0&0&0&0&0 \\ 0&0&0&0&0&0 \\ 0&0&0&0&0&0 \end{bmatrix}, \quad B_1 = B_2 = \begin{bmatrix} 0&0&0 \\ 0&0&0 \\ 0&0&0 \\ 1&0&0 \\ 0&1&0 \\ 0&0&1 \end{bmatrix} \tag{12}$$

The rotorcraft control problem is then, formulated as the control of two subsystems which are coupled by a nonlinear term $\Delta(u, \eta_d, e_\eta)$. The control objective is thus, to synthesize the control laws $\nu(\chi, \ddot{\xi}_d)$ and $\tilde{\tau}(e, \ddot{\eta}_d)$ such that the tracking errors χ and e will asymptotically converge to zero.

3. STABILITY OF SYSTEMS IN CASCADE

The idea behind the inner-outer loop control scheme is to design two independent controllers for the χ- and e-subsystem without considering the interconnection term $\Delta(\chi, e_\eta)$. As mentioned in the Introduction, this procedure simplifies the control design and results in simple and efficient control laws. However, the stability of the connected closed-loop system and its robustness with respect to $\Delta(\chi, e_\eta)$ have not been proven. Therefore, the first contribution of this paper is the analysis of the controller robustness with respect to the interconnection and coupling term $\Delta(\chi, e_\eta)$.

Much work has been done on the stability analysis of systems in cascade, Sontag (1988); Sepulcre et al. (1997). One of the most important theorem on the stability of systems in cascade is the following theorem expressed by Sontag (1988).

Theorem 2. If there is a feedback $\nu = \alpha(\chi, \ddot{\xi}_d)$ such that $\chi = 0$ is an asymptotically stable equilibrium of $\dot{\chi} = f(\chi, \alpha(\chi, \ddot{\xi}_d), \ddot{\xi}_d)$, then any partial state feedback control $\tilde{\tau} = \beta(e, \ddot{\eta}_d)$ which renders the e-subsystem equilibrium $e = 0$ asymptotically stable, also achieves asymptotic stability of $(\chi, e) = (0, 0)$. Furthermore, if the two subsystems are both Globally Asymptotically Stable (GAS), then, as $t \to \infty$, every solution $(\chi(t), e(t))$ either converges to $(\chi, e) = (0, 0)$ (GAS) or is unbounded.

Therefore, the stability of the connected system (11) will be ensured if we choose stabilizing feedbacks $\nu = \alpha(\chi, \ddot{\xi}_d)$, $\tilde{\tau} = \beta(e, \ddot{\eta}_d)$ and prove that all the trajectories $(\chi(t), e(t))$ are bounded.

One of the major tools usually used to show the boundedness of connected system trajectories is the Input-to-State-Stability (ISS) property, Sontag (1988). The ISS property is a strong condition which is often difficult to verify. For the system (11), the complexity is due to the interconnection term $\Delta(\chi, e_\eta)$. Consequently, we propose a theorem that guarantees the GAS of the connected system (11) provided that the interconnection term $\Delta(\chi, e_\eta)$ satisfies some relaxed conditions. This theorem is inspired by *Sepulcre*'s work, Sepulcre et al. (1997), Theorem 4.7, page 129.

Theorem 3. Let $\tilde{\tau} = \beta(e, \ddot{\eta}_d)$ be any C^1 partial-state feedback such that the equilibrium point $e = 0$ is GAS and LES. Suppose that there exist a positive constant c_1 and one class-$\mathcal{K}$ function $\gamma(.)$, differentiable at $e = 0$, such that

$$\|\chi\| \geq c_1 \Rightarrow \|\Delta(\chi, e_\eta)\| \leq \gamma(\|e_\eta\|)\, \|\chi\| \tag{13}$$

If there exist a positive semi-definite radially unbounded function $V(\chi)$ and positive constants c_2 and c_3 such that for $\|\chi\| \geq c_2$

$$\begin{cases} \dfrac{\partial V}{\partial \chi} f(\chi, \alpha(\chi, \ddot{\xi}_d), \ddot{\xi}_d) \leq 0 \\ \|\dfrac{\partial V}{\partial \chi}\|\, \|\chi\| \leq c_3 V(\chi) \end{cases} \tag{14}$$

then, the feedback $\tilde{\tau} = \beta(e, \ddot{\eta}_d)$ guarantees the boundedness of all the solutions of (11). Furthermore, if $\dot{\chi} = f(\chi, \alpha(\chi, \ddot{\xi}_d), \ddot{\xi}_d)$ is GAS, then the equilibrium point $(\chi, e) = (0, 0)$ is GAS.

Proof: The proof of Theorem 3 is given in Appendix A.

4. FLIGHT CONTROLLER DESIGN AND STABILITY

Here, we apply Theorem 2 to design a practical controller for the UAV transformed model given by (11). Theorem 3 is used to prove the asymptotic stability of the connected closed-loop system. The control design can thus, be achieved in three steps:

(1) Choose the control law $\nu = \alpha(\chi, \ddot{\xi}_d)$ that guarantees the Global Exponential Stability (GES) of the χ-subsystem without the interconnection term $\Delta(\chi, e_\eta)$.
(2) Choose the feedback $\tilde{\tau} = \beta(e, \ddot{\eta}_d)$, such that the e-subsystem is GES.

(3) Prove that the system (11) satisfies the conditions stated in Theorem 3. In fact, we need to prove that the interconnection term $\Delta(\chi, e_\eta)$ satisfies the growth condition (13).

Since the χ- and e-subsystems are linear, we can use simple linear controllers such as PD or PID. Therefore, we synthesize two control laws

$$\begin{cases} \nu = -K_\chi \chi + \ddot{\xi}_d, \ K_\chi \in \mathbb{R}^{3\times 6} \\ \tilde{\tau} = -K_e e + \ddot{\eta}_d, \ K_\chi \in \mathbb{R}^{3\times 6} \end{cases} \tag{15}$$

such that the matrices $A_\chi = A_1 - B_1 K_\chi$ and $A_e = A_2 - B_2 K_e$ are Hurwitz.

By substituting (15) into (11), the closed-loop system is given by

$$\begin{cases} \dot{\chi} = A_\chi \chi + \Delta(\chi, e_\eta) \\ \dot{e} = A_e e \end{cases} \tag{16}$$

Although A_χ and A_e are Hurwitz, the asymptotic stability of the closed-loop system (16) can not be directly deduced because of the interconnection term $\Delta(\chi, e_\eta)$. Thus, we apply Theorem 3 in order to prove the asymptotic stability of the connected closed-loop system (16).

Since A_χ and A_e are Hurwitz, the χ-subsystem (without the interconnection term) and the e-subsystem are GES which is stronger than the GAS property. The GES of the χ-subsystem implies that there exist a positive definite radially unbounded function $V(\chi)$ and positive constants c_2 and c_3 such that for $\|\chi\| \geq c_2$: $\frac{\partial V}{\partial \chi} A_\chi \chi \leq 0$ and $\|\frac{\partial V}{\partial \chi}\| \|\chi\| \leq c_3 V(\chi)$. Therefore, the condition (14) of Theorem 3 is satisfied.

Now, it remains to show that the interconnection term $\Delta(\chi, e_\eta)$ satisfies the growth restriction (13) of Theorem 3. The norm of the interconnection term $\Delta(\chi, e_\eta)$ can be expressed as follows:

$$\|\Delta(\chi, e_\eta)\| = \frac{1}{m}|u(\chi)| \|H(\chi, e_\eta)\| = \frac{1}{m}|u(\chi)| \sqrt{h_x^2 + h_y^2 + h_z^2} \tag{17}$$

where (h_x, h_y, h_z) are defined in (9) and

$$|u(\chi)| = m\|\nu(\chi) + g e_3\| = m\sqrt{\nu_x^2 + \nu_y^2 + (\nu_z + g)^2}$$

Before proving the boundedness of the interconnection term $\Delta(\chi, e_\eta)$, we need the following two lemmas:

Lemma 4. Assume that the desired trajectories $\xi_d(t)$ and their time-derivatives are bounded and denote $L_d = \|\ddot{\xi}_d\|_\infty$. Then, there exist positive constants r and k_1 such that the collective thrust feedback $u(\chi)$ satisfies the following properties:

$$|u(\chi)| \leq \begin{cases} k_1 \|\chi\|, & \text{for } \|\chi\| \geq r \\ k_1 r, & \text{for } \|\chi\| < r \end{cases} \tag{18}$$

Lemma 5. There exists a positive constant k_2 such that the coupling term $H(\chi, e_\eta)$ satisfies the following inequality:

$$\|H(\chi, e_\eta)\| \leq k_2 \|e_\eta\| \tag{19}$$

The proofs of Lemmas 4 and 5 are given in Appendix B.

From Lemmas 4 and 5, we can write that for $\|\chi\| \geq r$, we have

$$\|u\ H(.)\| \leq k_1 \|\chi\|\ k_2 \|e_\eta\| = k \|e_\eta\| \|\chi\| \tag{20}$$

where $k = k_1\ k_2$ is a positive constant.

Finally, we obtain the following inequality

$$\|\Delta\| = \frac{1}{m}\|u\ H\| \leq \gamma(\|e_\eta\|)\|\chi\|, \ \text{ for } \|\chi\| \geq r \tag{21}$$

where $\gamma(.) = \frac{k}{m}\|e_\eta\|$ is a class-$\mathcal{K}$ function.

So, all the conditions of Theorems (2)-(3) are satisfied and the GAS of the equilibrium point $(\chi, e) = (0, 0)$ is then guaranteed.

We have synthesized two practical control laws for controlling the rotorcraft position and orientation. By exploiting the theory of systems in cascade, we have proven the GAS of the rotorcraft model given by (5). The block diagram of the overall controller is shown in Fig. 1.

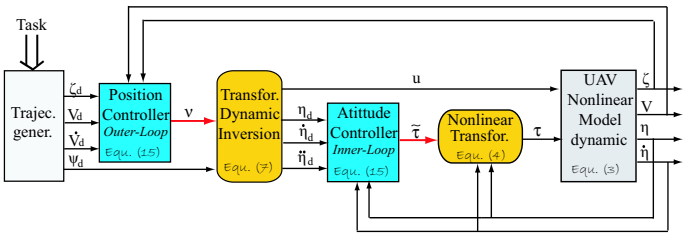

Fig. 1. Structure of the inner-outer loop-based controller

5. SIMULATION RESULTS

In order to evaluate the performance of the designed flight controller, we have performed two tests by considering the nonlinear model of the rotorcraft. Furthermore, white noise has been added to the measurements. Indeed, a zero-mean noise with 0.01 variance has been added to the position and velocity signals, and the attitude measurements have been corrupted by a noise of 0.0001 variance. The considered initial conditions are $\xi(0) = (5, 1, 10)^T, \upsilon(0) = (1, -1, 0)^T, \eta(0) = (-0.1, 0.3, 0.5)^T$ and $\dot{\eta}(0) = (0, 0, 0)^T$.

In the first experiment, the rotorcraft UAV was tasked to stabilize its attitude and horizontal movement and achieve a smooth landing. From Figs. 2 and 3 we can see that

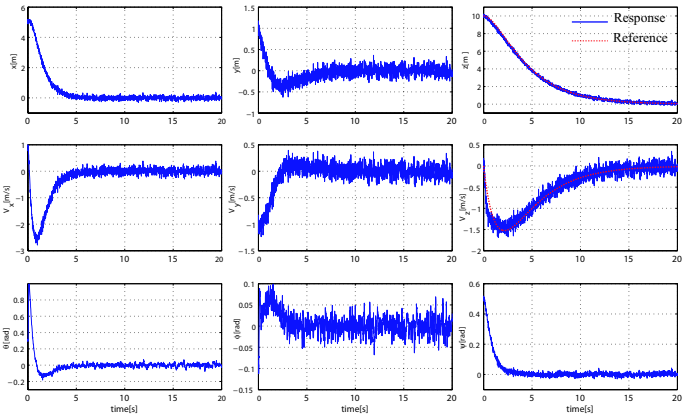

Fig. 2. Rotorcraft stabilization and landing using noisy measurements

control objective is successfully achieved.

In the second experiment, the control objective was to make the aircraft track an aggressive 3D trajectory. As

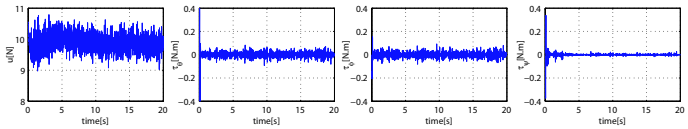

Fig. 3. Control inputs (stabilization)

shown in Fig. 6, the rotorcraft was tasked to take off elliptically, and then to achieve a circular flight at a desired altitude of 25 m, followed by a hover flight and finally to land vertically. Significant noise and external disturbances $F_{ext} = (0.5, 0.5, 0.5\ N)^T$ have been added to the rotorcraft model. It can be seen that the controller

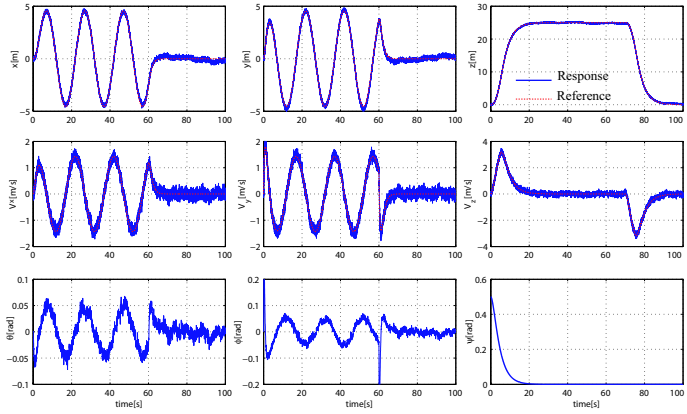

Fig. 4. Trajectory tracking: take-off, circular flight, hovering and vertical landing

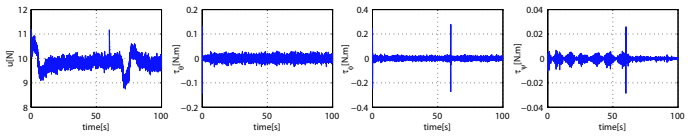

Fig. 5. Control inputs (trajectory tracking)

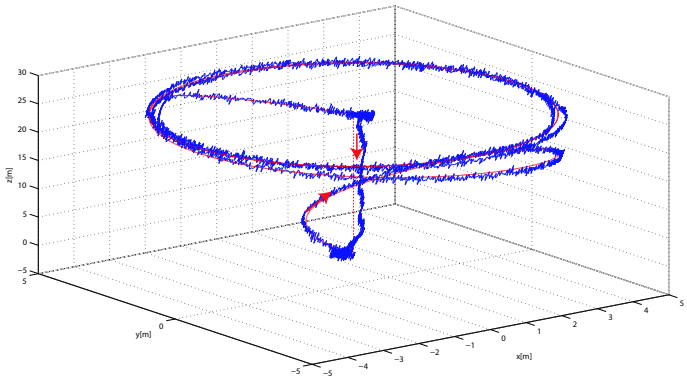

Fig. 6. 3D trajectory of the rotorcraft UAV

performs very well and it is robust with respect to noise and external perturbations. Figs. 4-6 show the position, attitude, control inputs and the UAV 3D trajectory. The assigned navigational task was successfully achieved and the reference trajectories were tracked with high accuracy.

6. CONCLUSION

In this paper, we have presented a practical flight controller that exploits the model structure of rotorcraft UAVs. The aircraft dynamics are modelled by two connected subsystems. In fact, we have applied dynamic inversion to the position subsystem and feedback linearization to the rotation dynamics, thereby resulting in two linear subsystems connected by a complex nonlinear term. Two control laws have been then, synthesizing for controlling the UAV position (outer-loop) and orientation (inner-loop). The asymptotic stability property has been proven for the connected closed-loop system, and the performance of the proposed hierarchical controller has been observed in simulations.

REFERENCES

S. Bouabdallah, A. Noth, and R. Siegwart. PID vs LQ control techniques applied to an indoor micro quadrotor. In *Proc. of the IEEE/RSJ Int. Conf. on Intelligent Robots and Systems*, pages 2451–2456, Sendai, Japan, 2004.

T. Hamel, R. Mahony, R. Lozano, and J. Ostrowski. Dynamic modelling and configuration stabilization for an X4-flyer. In *Proc. of the 15th IFAC World Congress*, Barcelona, Spain, 2002.

E.N. Johnson and S.K. Kannan. Adaptive trajectory control for autonomous helicopters. *AIAA Journal of Guidance, Control, and Dynamics*, 28(3):524–538, May-June 2005.

F. Kendoul, I. Fantoni, and R. Lozano. Modeling and control of a small autonomous aircraft having two tilting rotors. *IEEE Transactions on Robotics*, 22(6):1297–1302, December 2006.

F. Kendoul, D. Lara, I. Fantoni, and R. Lozano. Real-time nonlinear embedded control for an autonomous quadrotor helicopter. *AIAA Journal of Guidance, Control, and Dynamics*, 30(4):1049–1061, 2007.

T.J. Koo and S. Sastry. Output tracking control design of a helicopter model based on approximate linearization. *In Proc. of the IEEE Conf. on Decision and Control*, pages 3635–3640, Florida, USA, December 1998.

Ma. La Civita, G. Papageorgiou, W. C. Messner, and T. Kanade. Design and flight testing of an H_∞ controller for a robotic helicopter. *AIAA Journal of Guidance, Control, and Dynamics*, 29(2):485–494, April 2006.

R. Mahony and T. Hamel. Robust trajectory tracking for a scale model autonomous helicopter. *Int. J. of Robust and Nonlinear Control*, 14(12):1035–1059, 2004.

K. Nonami. Fully autonomous unmanned small-scale helicopter and micro air vehicle control. In *Proc. of the 8th Inter. Conf. on Motion and Vibration Control (MOVIC 2006*, Korea, August, 2006.

R. Olfati-Saber. Nonlinear control of underactuated mechanical systems with application to robotics and aerospace vehicles. *PhD Thesis Report, Department of Electrical Engineering and Computer Science, MIT, USA*, 2001.

M. Oosterom and R. Babuska. Design of a gain-scheduling mechanism for flight control laws by fuzzy clustering. *Control Engineering Practice*, 14(7):769–781, 2006.

J. Reiner, G.J. Balas, and W.L. Garrard. Robust dynamic inversion for control of highly maneuverable aircraft. *AIAA Journal of Guidance, Control, and Dynamics*, 18 (1):18–24, 1995.

R. Sepulcre, M. Jankovic, and P. Kokotovic. *Constructive Nonlinear Control.* Communications and Control

Engineering Series. Springer-Verlag, 1997.
E.D. Sontag. Smooth stabilization implies coprime factorization. *IEEE Trans. on Automatic Control*, 34(4): 435–443, 1988.

Appendix A. PROOF OF THEOREM 2

Let $(\chi(0), e(0))$ be an arbitrary initial condition, and let $V(\chi)$ be a semi-definite positive function. By recalling (13) and (14), then for $\|\chi\| \geq \max(c_1, c_2)$ we have the following inequalities:

$$\dot{V}(\chi) = \underbrace{\frac{\partial V}{\partial \chi} f(.)}_{\leq 0} + \frac{\partial V}{\partial \chi}\Delta(.) \leq \frac{\partial V}{\partial \chi}\Delta(.) \leq \|\frac{\partial V}{\partial \chi}\|\|\Delta\|$$
$$\leq \|\frac{\partial V}{\partial \chi}\|\gamma(\|e_\eta\|)\|\chi\| \leq c_3 V(\chi)\gamma(\|e_\eta\|) \qquad (A.1)$$

Since the equilibrium point $e_\eta = 0$ is GAS and LES, then $\|e_\eta\|$ converges to zero exponentially. This implies that

$$\gamma(\|e_\eta(t)\|) \leq \gamma(\|e_\eta(0)e^{-at}\|) \leq \gamma_1(\|e_\eta(0)\|)e^{-at}$$

with a is a positive constant and $\gamma_1(.)$ is a class-$\mathcal{K}$ function.

Now, the derivative of $V(\chi)$ satisfies

$$\dot{V}(\chi) \leq c_3 V(\chi)\ \gamma_1(\|e_\eta(0)\|)\ e^{-at},\ \text{ for } \|\chi\| \geq \max(c_1, c_2)$$

We define a positive constant c as: $c = c_3\ \gamma_1(\|e_\eta(0)\|)$.

$$\text{Thus: } \dot{V}(\chi) \leq cV(\chi)\ e^{-at},\ \text{ for } \|\chi\| \geq \max(c_1, c_2)$$

This relation proves the boundedness of $V(\chi)$ because

$$V(\chi) \leq V(\chi(0))\ e^{\int_0^t c\, e^{-as}\, ds} \leq \gamma_2(\|e_\eta(0)\|)V(\chi(0))$$

for some $\gamma_2(.) \in \mathcal{K}$.

Because $V(\chi)$ is radially unbounded, the boundedness of $V(\chi)$ implies the boundedness of $\|\chi\|$.

Therefore, the GAS of the equilibrium point $(\chi, e) = (0, 0)$ follows from Theorem 2.

Remark 6. In the previous analysis, the boundedness of $\|\chi\|$ was proven for $\|\chi\| \geq \max(c_1, c_2)$. If $\|\chi\| < \max(c_1, c_2)$, then its boundedness is satisfied by the assumption itself.

Appendix B. PROOFS OF LEMMAS 1 AND 2

B.1 Boundedness of $|u(\chi)|$

Let us recall the expressions of the thrust u and the feedback ν.

$$\begin{cases} |u(\chi)| = m\|\ \nu(\chi, \ddot{\xi}_d) + g e_3\| \\ \nu(\chi, \ddot{\xi}_d) = -K_\xi \chi_\xi - K_v \chi_v + \ddot{\xi}_d \end{cases} \qquad (B.1)$$

Let $\lambda_\xi > 0$ and $\lambda_v > 0$ be the maximum values of K_ξ and K_v eigenvalues respectively. Thus, we write

$$|u(\chi)| = m\|g e_3 + \ddot{\xi}_d - K_\xi \chi_\xi - K_v \chi_v\|$$
$$\leq m(g + \|\ddot{\xi}_d\| + \lambda_\xi\|\chi_\xi\| + \lambda_v\|\chi_v\|)$$
$$\leq m(g + L_d + \ \max(\lambda_\xi, \lambda_v)(\|\chi_\xi\| + \|\chi_v\|))$$
$$\leq m(g + L_d) + m\ \max(\lambda_\xi, \lambda_v)\sqrt{2}\|\chi\|$$

because

$$(\|\chi_\xi\| + \|\chi_v\|)^2 = \|\chi_\xi\|^2 + \|\chi_v\|^2 + 2\|\chi_\xi\|\|\chi_v\| \leq$$
$$2(\|\chi_\xi\|^2 + \|\chi_v\|^2),\ \text{ which implies that}$$
$$\|\chi_\xi\| + \|\chi_v\| \leq \sqrt{2}\sqrt{\|\chi_\xi\|^2 + \|\chi_v\|^2} = \sqrt{2}\|\chi\|$$

Setting $c \triangleq m\sqrt{2}\ \max(K_\xi, K_v)$, we get

$$|u(\chi)| \leq m(g + L_d) + c\|\chi\| \leq c(\frac{mg + mL_d}{c} + \|\chi\|)$$
$$\leq c(r + \|\chi\|), \quad \text{where } r = \frac{mg + mL_d}{c}$$

From the above inequalities, we deduce that

$$|u(\chi)| \leq \begin{cases} k_1\|\chi\|, \text{ for all} \|\chi\| \geq r \\ k_1 r, \quad \text{for all} \|\chi\| < r, \ \text{ where } k_1 = 2c \end{cases} \qquad (B.2)$$

B.2 Boundedness of $\|H(.)\|$

We had $\|H(\chi, e_\eta)\| = \sqrt{h_x^2 + h_y^2 + h_z^2}$ where the expressions of the components (h_x, h_y, h_z) are given in (9) and verify:

$$\begin{aligned} |h_x| &\leq |\sin(e_\theta/2)| \\ |h_y| &\leq |\sin(e_\phi/2)||\sin(e_\theta/2)| + |\sin(e_\theta/2)| + |\sin(e_\phi/2)| \\ |h_z| &\leq |\sin(e_\phi/2)||\sin(e_\theta/2)| + |\sin(e_\theta/2)| + |\sin(e_\phi/2)| \end{aligned} \qquad (B.3)$$

Let us recall some trivial inequalities

$$|\sin a| \leq |a| \qquad (B.4)$$
$$|a||b| \ \leq \frac{1}{2}(|a| + |b|),\ \text{for } |a| \leq 1 \text{ and } |b| \leq 1 \qquad (B.5)$$

Then, we can write

$$|h_x| \leq \frac{1}{2}|e_\theta|$$
$$|h_y| \leq \frac{3}{2}(|\sin(e_\theta/2)| + |\sin(e_\phi/2)|) \leq \frac{3}{4}(|e_\theta| + |e_\phi|)$$
$$|h_z| \leq \frac{3}{2}(|\sin(e_\theta/2)| + |\sin(e_\phi/2)|) \leq \frac{3}{4}(|e_\theta| + |e_\phi|)$$

By computing the squares of the previous functions, we obtain

$$h_x^2 \leq \frac{1}{4}e_\theta^2$$
$$h_y^2 \leq \frac{9}{16}(e_\theta^2 + e_\phi^2 + 2|e_\theta||e_\phi|)$$
$$h_z^2 \leq \frac{9}{16}(e_\theta^2 + e_\phi^2 + 2|e_\theta||e_\phi|)$$

Note that $2|e_\theta||e_\phi| \leq e_\theta^2 + e_\phi^2$. Thus,

$$h_x^2 \leq \frac{1}{4}e_\theta^2;\ h_y^2 \leq \frac{9}{8}(e_\theta^2 + e_\phi^2);\ h_z^2 \leq \frac{9}{8}(e_\theta^2 + e_\phi^2) \qquad (B.6)$$

From (B.6), we deduce that

$$\|H(.)\| \leq \sqrt{\frac{10}{4}e_\theta^2 + \frac{9}{4}e_\phi^2} \leq \sqrt{\frac{10}{4}(e_\theta^2 + e_\phi^2)} \qquad (B.7)$$
$$\leq k_2\|e_\eta\| \ \text{ with } k_2 = \frac{\sqrt{10}}{2} \qquad (B.8)$$

and this ends the proof.